

CompoNeRF: Text-guided Multi-object Compositional NeRF with Editable 3D Scene Layout

Haotian Bai¹, Yuanhuiyi Lyu¹, Lutao Jiang¹, Si Jia Li², Haonan Lu², Xiaodong Lin², Lin Wang^{1,3†}

¹VLIS LAB, AI Thrust, HKUST(GZ) ²OPPO ³Dept. of CSE, HKUST

haotianwhite@outlook.com, yuanhuiyilv@hkust-gz.edu.cn, jiangluta098@gmail.com, {lisijia, luhaonan, linxiaodong}@oppo.com, linwang@ust.hk

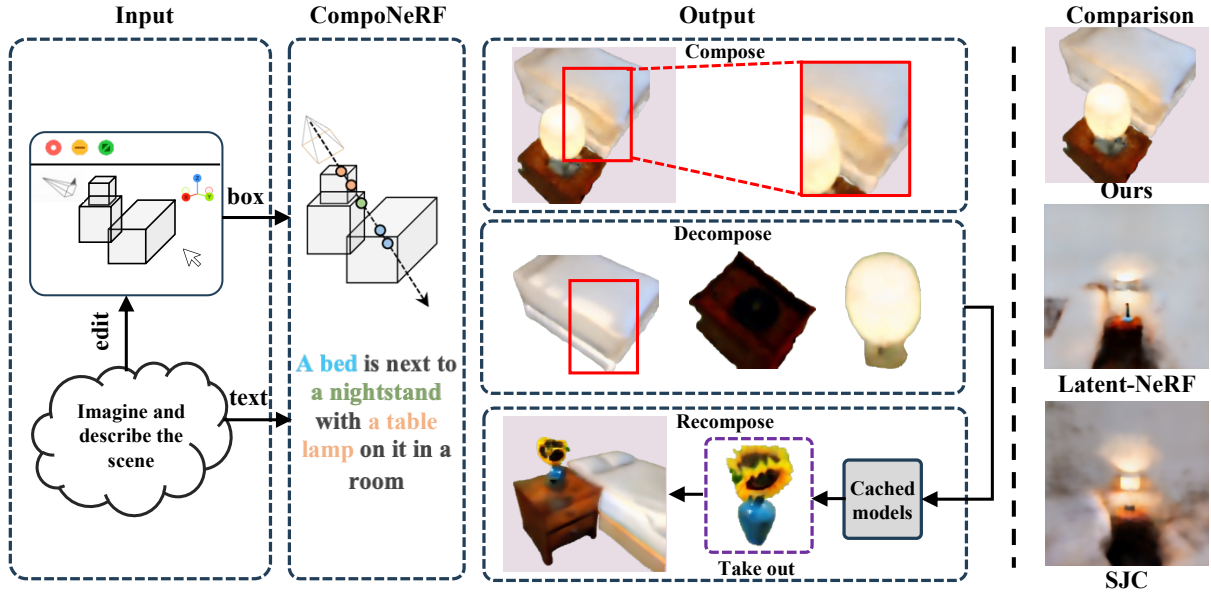


Figure 1: **Left:** We introduce CompoNeRF, a method that uses boxes and texts to *compose* NeRFs with global consistency.(e.g., the global reflection highlighted in red). Besides its accuracy, each NeRF model can be *decompose* and edited to *recompose* large scenes effectively. **Right:** Despite recent efforts to develop text-to-3D generation, represented by works such as Latent-NeRF (Metzer et al. 2022) and SJC (Wang et al. 2022b), they often struggle to understand long sentences in our daily lives and usually fail to produce desired results in terms of number, type, and quality.

Abstract

Recent research endeavors have shown that combining neural radiance fields (NeRFs) with pre-trained diffusion models holds great potential for text-to-3D generation. However, a hurdle is that they often encounter guidance collapse when rendering multi-object scenes with relatively long sentences. Specifically, text-to-image diffusion models are inherently unconstrained, making them less competent to accurately associate object semantics with 3D structures. To address it, we propose a novel framework, dubbed **CompoNeRF**, to explicitly incorporate an editable 3D scene layout to provide effective guidance at the object (*i.e.*, local) and scene (*i.e.*, global) levels. Firstly, we interpret the multi-object text as an editable 3D scene layout containing multiple local NeRFs associated with the object-specific 3D boxes and text prompt. Then, we introduce a composition module to calibrate the latent features from local NeRFs, which surprisingly improves

the view consistency across different local NeRFs. Lastly, we apply text guidance on global and local levels through their corresponding views to avoid guidance ambiguity. Additionally, NeRFs can be decomposed and cached for composing other scenes with fine-tuning. This way, our CompoNeRF allows for flexible scene editing and recomposition of trained local NeRFs into a new scene by manipulating the 3D layout or text prompt. Leveraging the open-source Stable Diffusion model, our CompoNeRF can generate faithful and editable text-to-3D results while opening a potential direction for text-guided multi-object composition via the editable 3D scene layout. Notably, our CompoNeRF can achieve at most **54%** performance gain based on the CLIP score metric. Code is available at <https://>.

1 Introduction

Recently, text-to-image generation has achieved tremendous success by coupling the vision-language pre-trained models (Radford et al. 2021; Li et al. 2022) with diffusion

† Corresponding author

models (Ho, Jain, and Abbeel 2020; Nichol and Dhariwal 2021; Rombach et al. 2022). These breakthroughs have also yielded far-reaching implications in text-to-3D generation (Jain et al. 2022; Sanghi et al. 2022; Hong et al. 2022; Gao et al. 2022; Mohammad Khalid et al. 2022; Lee and Chang 2022; Xu et al. 2022a) using powerful vision-language pre-trained models. More recently, several text-to-3D methods (Poole et al. 2022; Lin et al. 2022; Metzer et al. 2022; Wang et al. 2022b) have shown that matching the rendered views from the differential 3D model, such as Neural Radiance Fields (NeRFs) (Mildenhall et al. 2020a; Barron et al. 2021; Müller et al. 2022), with the learned text-to-image distribution from pre-trained diffusion model can produce remarkable results.

However, the textual description is often an abstract specification for a desired target 3D model or a 2D image. Despite that the powerful diffusion models, *e.g.*, Stable Diffusion (Rombach et al. 2022), have been trained on billions of text-image pairs (Schuhmann et al. 2022), it is still a challenge to generate geometrically coherent images across different viewpoints from the text. Moreover, the diffusion model may produce inaccurate results (Feng et al. 2022) given text containing multiple objects, resulting in missing objects or semantic confusion. For example, Fig. 2 demonstrates that Stable Diffusion fails to maintain object identities and geometric coherence even with a simple multi-object text. It obviously contradicts the essence of volume rendering in NeRF, leading to a hurdle —*guidance collapse*, especially when rendering multi-object scenes with text prompts. As a result, state-of-the-art (SoTA) Latent-NeRF (Metzer et al. 2022) and SJC (Wang et al. 2022b) models can only generate part of concepts in the multi-object text shown in Fig. 2, limiting their application for object-compositional 3D scene generation from text prompts.

Therefore, it naturally raises the question: *whether the agnostic distribution of the diffusion model can accurately learn and compose all the concepts in a multi-object text for 3D scene generation*. According to Fig. 2, we observe that the diffusion model can more accurately generate single objects with their respective local text prompts. This motivates us to introduce more fine-grained text guidance to tackle the guidance collapse issue in existing frameworks (Metzer et al. 2022; Wang et al. 2022b) when using multi-object text prompts. Thus, a straightforward solution is to bind object-oriented guidance to each object, making the 3D representation and rendering pipeline object-aware. However, existing approaches (Poole et al. 2022; Lin et al. 2022; Metzer et al. 2022; Wang et al. 2022b) tend to use a single neural network to encode the entire scene, making it hard to incorporate the decomposed guidance during training as they are generally agnostic to the object’s identity and quantity.

Inspired by this observation, we propose a compositional NeRF framework, called **CompoNeRF**, interpreting multi-object text guidance as an editable 3D scene boxes with fine-grained text prompts. The scene layout collects individual object entities from the input text and gathers their editable 3D bounding boxes as shown in Fig. 1. In CompoNeRF, each box in the 3D scene layout is modeled by a local NeRF for representation learning, and global views are rendered

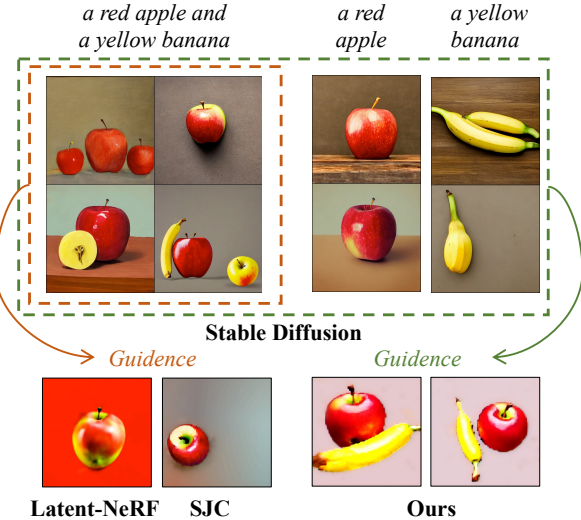


Figure 2: **The guidance collapse issue** on generating multi-object scenes by Stable Diffusion. we observe that using both global and local text guidance can mitigate this issue.

by compositing the learned 3D representations from local NeRFs. However, direct composition from all local NeRFs may not ensure coherent global views without addressing the following two issues.

1) Independence: capturing consistent global views across multiple local NeRFs is hard due to non-shared parameters. To solve this, we use a global MLP to calibrate the local NeRF predictions based on their samples’ global coordinates and ray directions. The model can gradually learn global consistency across multiple objects by passing the global constraint into local NeRFs.

2) Occlusion: inaccurate text guidance may result from fully occluded objects due to random camera positions in the training data. To tackle the occlusion issue, we employ local text guidance on every individual NeRF-rendered view. Thanks to the use of the diffusion model, we are able to provide precise guidance for object identification even in the presence of occlusion. As a result, our approach ensures coherent and realistic 3D generation, even in crowded scenes that include multiple objects as depicted in Fig. 1 without object missing or text ambiguity.

Moreover, scene editing is facilitated by the use of 3D scene layout, allowing flexible manipulation of text and objects, including scaling, movement, and removal. Using a vast pre-trained content gallery, we can rapidly generate desired 3D scenes with text prompts and layouts, democratizing 3D content creation. The comparisons of related approaches are summarized in Tab. 1. Additionally, previous studies fail to include a quantitative comparison, resulting in inadequate evaluation relying solely on visual comparison. We thus propose to employ the extensively recognized CLIP score (Wang et al. 2022a) to assess the efficiency of generating 3D models from text descriptions. By doing so, we provide a more comprehensive demonstration of our proficiency in producing intricate multi-object scenes.

Methods	Diffusion Model	3D Representation	Scene Rendering	Input Prompt	Scene Editing	recomposition
DreamFusion	Imagen	Mip-NeRF 360	Object-centric	Text	T	✗
Magic3D	eDiff-I + SD	Instant-NGP	Object-centric	Text	T	✗
DreamBooth3D	DreamBooth+DreamFusion	Mip-NeRF	Object-centric	Text+Images	T	✗
Points-to-3D	ControlNet+Point-E	Instant-NGP	Object-centric	Text+Image	T	✗
Latent-NeRF	SD	Instant-NGP	Object-centric	Text+Fine Shape	T	✗
SJC	SD	voxel radiance field	Object-centric	Text	T	✗
Ours	SD	Instant-NGP	Object-compositional	Text+3D Coarse Boxes	T/M/S/R	✓

Table 1: **Comparison of our method with the related works for text-to-image generation.** SD denotes Stable Diffusion. For scene editing, we use T(editing object with text), M(moving object), S(scaling object), and R(remove object) for short.

To summarize, our paper makes three key contributions: **(I)** We solve the guidance collapse issue in multi-object 3D scene generation by integrating an editable 3D layout with multiple local NeRFs to precisely associate guidance with specific objects. Additionally, all local NeRFs can be cached, edited and reused for composing other scenes. **(II)** We address the issues of independence and occlusion by using composition module to calibrate the overall rendering and varying levels of text guidance to maintain the identity of individual entities while ensuring global coherence. **(III)** We thoroughly evaluate the effectiveness of our proposed method across various multi-object scenarios, demonstrating its ability to composite and edit 3D scenes via qualitative and quantitative analysis. We propose to use CLIP score as the metric to evaluate the similarity of the generated 3D assets to the prompt text, and our CompoNeRF achieves the best performances on various multi-object scenes.

2 Related Work

Text-guided 3D Generative Models. Motivated by the success of the vision-language models, *e.g.*, CLIP (Radford et al. 2021), text-guided 3D generation has also been rapidly progressing. Several works (Jain et al. 2022; Wang et al. 2022a; Mohammad Khalid et al. 2022; Sanghi et al. 2022; Xu et al. 2022a) utilize the pre-trained vision-language model to provide robust alignment between image features extracted from rendered views of 3D representations and text features by minimizing feature similarity. Though pre-trained large-scale vision-language models can offer strong 2D guidance for 3D representation learning, the quality of their 2D rendering results may be less realistic due to insufficient details in the features. Recently, DreamFusion (Poole et al. 2022) demonstrates remarkable capability in text-to-3D object generation by incorporating a powerful pre-trained text-to-image diffusion model (Saharia et al. 2022) through score distillation sampling. Similarly, Magic3D (Lin et al. 2022) proposes a two-stage super-resolution method to enhance generation quality with hybrid 3D representation. Latent-NeRF (Metzer et al. 2022) demonstrates that updating NeRF in the latent space using score distillation sampling can also produce realistic results. SJC (Wang et al. 2022b) improves the sampling process by introducing a perturb-and-average scoring scheme to address distribution mismatching issues. DreamBooth3D (Raj et al. 2023) proposes a three-stage method that utilizes DreamBooth (Ruiz et al. 2023)

and DreamFusion to generate 3D object from the text and 3-6 images inputs. Points-to-3D (Yu et al. 2023) utilizes the sparse 3D point cloud as the immediate representation to guide the 3D generative NeRF model.

By contrast, our CompoNeRF generates multi-object 3D scenes in an *object-compositional* way by utilizing multiple local NeRFs to model the scene instead of a holistic object-centric representation. Our editable 3D scene layout allows for editing of scenes by changing the text prompt similarly as (Poole et al. 2022; Lin et al. 2022). Also, it enables manipulation of the spatial arrangement of individual objects in a crowded scene, as summarized in Tab. 1. Moreover, the layout allows for recomposition with other off-the-shelf representations, enabling the rapid generation of new scenes.

Neural Rendering for 3D Modeling. The advancement of NeRF has greatly improved the performance of neural renderers. NeRF models (Mildenhall et al. 2020b; Lindell, Martel, and Wetzstein 2021; Müller et al. 2022; Liu et al. 2020; Barron et al. 2021; Verbin et al. 2022; Zhang et al. 2020) are a family of volume rendering algorithms that utilize coordinate-based MLPs to directly predict color and opacity from the 3D position and 2D viewing direction. The photo-realistic synthesized views from these models have led to the widespread adoption of differential volume rendering in various applications, *e.g.*, relighting (Srinivasan et al. 2021; Zhang et al. 2021), dynamic scene reconstruction (Gao et al. 2021; Pumarola et al. 2021; Xian et al. 2021; Tretschk et al. 2021), editable scenes and avatars (Liu et al. 2021; Yang et al. 2021), and surface reconstruction (Ažinović et al. 2022; Wang et al. 2021). These methods commonly use *single* MLP to encode the entire scene, which can be ambiguous *w.r.t.* specific object identities within the scene. Note that our method involves rendering the scene using multiple local NeRFs, and the rendering process requires compositing all the local NeRF predictions based on their spatial relationships.

Object-Compositional Scene Modeling. The idea of generating new scenes by compositing multiple object-centric representations is a straightforward approach in scene generation (Guo et al. 2020). Several works (Zhi et al. 2021; Yang et al. 2021; Wu et al. 2022; Mirzaei et al. 2022; Niemeyer and Geiger 2021; Ost et al. 2021; Xu et al. 2022b; Song et al. 2022) attempt to directly decompose object representations from the scene image to perform compositional scene modeling. Based on the additional object-level information, they can be roughly categorized as semantic based (Zhi

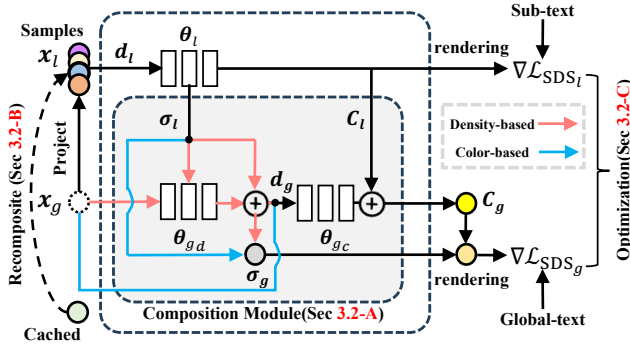


Figure 3: **Framework Overview.** Our model consists of two branches where the upper part is individual NeRFs, and the lower part denotes global calibration with our tailored composition model. The specific designs for density-based and color-based composition modules are highlighted, while the black ones are shared for the two options.

et al. 2021; Yang et al. 2021; Wu et al. 2022; Mirzaei et al. 2022; Niemeyer and Geiger 2021) and 3D layout based (Ost et al. 2021; Xu et al. 2022b; Song et al. 2022). Semantic based methods incorporate extra semantic information, such as segmentation labels (Zhi et al. 2021), object instance mask (Yang et al. 2021; Wu et al. 2022), and features from the pre-trained vision-language model (Mirzaei et al. 2022), to learn the object representations. On the other hand, 3D layout-based methods directly use the 3D object coordinate information as the object guidance for learning object-specific representation and generating the full scene by compositing all object representations. For instance, NSG (Ost et al. 2021) and its variant (Song et al. 2022) use a scene graph structure to model dynamic scenes, associating each object with a 3D box and a node representation. While previous works focused on decomposing object entities from real-world images, our work serves as the *first* attempt to tackle the text-to-3D generation via decomposed representations with 3D scene layout.

3 Methodology

To resolve the issue of guidance collapse, our core idea is to *decompose the scene into reusable components and compose/recompose them into a globally consistent one*. This enables flexible control over the generated content with simple prompts and box layouts, as illustrated in Fig. 1. Our proposed CompoNeRF offers the following advantages: 1) **semantic coherence**: we generate 3D objects precisely with rich texture and global consistency, such as realistic light reflection on the bed. 2) **disassembly and reusability**: CompoNeRF is a collection of individually trained NeRF models that can be saved and reloaded from the off-the-shelf dataset. 3) **editability**: our method support recomposition by placing NeRF models at the arbitrary scene positions, *e.g.*, replacing the lamp with a vase of sunflowers or adjusting object size by simply scaling their bounding boxes.

3.1 Preliminaries

Referring to individual boxes as *local frames*, and the global scene space as the *global frame*, we introduce both preliminaries on NeRF and diffusion here.

3D Representation in Latent Space. Our approach is built upon SoTA text-to-image model—Stable Diffusion (Rombach et al. 2022). To avoid heavy pixel computations, we rely on Latent-NeRF (Metzer et al. 2022) to infer pseudo-color for each object using local NeRF. Specifically, the representation maps a point $x_l = (x_l, y_l, z_l) \in [-1, 1]$ in the local frame to its corresponding volumetric density σ_l and emitted color C_l , *i.e.*, $(C_l, \sigma_l) = \theta_l(x_l, y_l, z_l)$. The predicted pseudo-color is fed forward into the decoder of the Stable Diffusion model to obtain the final rendering result.

Volume Rendering with Multiple Objects. For each local frame j with NeRF parameterized as θ_j , we follow original NeRF design (Mildenhall et al. 2020b) to integrate (C_l, σ_l) of sampled points from any hit ray $r_l = (o_l, d_l)$ by,

$$\hat{C}_l(r_l) = \sum_{k=1}^N T_k (1 - \exp(-\sigma_{l,k} \delta_k)) C_{l,k}, \quad (1)$$

where o_l is the camera center that emits rays with direction d_l . For a batch of rays r , the light transmittance to sample i is denoted as $T_k = \exp\left(-\sum_{j=1}^{k-1} \sigma_{l,j} \delta_j\right)$, δ_k is the distance between adjacent samples, \hat{C}_l is the predicted color, and N is the number of samples within each ray interval.

For consistent scene rendering, object transmittance T_k must be recalculated in the global frame based on independent properties inferred from local NeRFs. Hence, we sort predictions according to their distance to o_g . Similar to Eq. (1), global color \hat{C}_g of ray $r_g = (o_g, d_g)$ is predicted by the volumetric rendering integrating over m objects,

$$\hat{C}_g(r_g) = \sum_{k=1}^{m*N} T_k (1 - \exp(-\sigma_{g,k} \delta_k)) C_{g,k}. \quad (2)$$

Score Distillation Sampling. To achieve text-to-3D generation, DreamFusion (Poole et al. 2022) introduces Score Distillation Sampling (SDS) to propagate the text-to-image generative prior from diffusion model ϕ to the NeRF parameters θ . During the SDS process, a noise image \mathbf{X}_t is first generated by adding a sampled noise $\epsilon \sim \mathcal{N}(0, I)$ in noise level t into a rendered view \mathbf{X} from a NeRF. Then, the diffusion model ϕ predicts the sampled noise $\epsilon_\phi(\mathbf{X}_t, t, T)$ given the noisy image \mathbf{X}_t , noise level t , and optional text prompt T . Specifically, SDS computes the gradient from the distance between the predicted and added noises,

$$\nabla_\theta \mathcal{L}_{SDS}(\mathbf{X}_t, T) = w(t) (\epsilon_\phi(\mathbf{X}_t, t, T) - \epsilon), \quad (3)$$

where $w(t)$ is a weighting function. The gradient direction generated on all rendered views is used to update θ to match images conditioned on text prompt under diffusion prior. We also follow SJC (Wang et al. 2022b) to apply the perturb and average scoring into SDS. Please refer to (Poole et al. 2022; Wang et al. 2022b) for the complete details.

3.2 The Proposed CompoNeRF

A. Composition Module CompoNeRF aims to composite multiple NeRFs to reconstruct multi-object scenes with

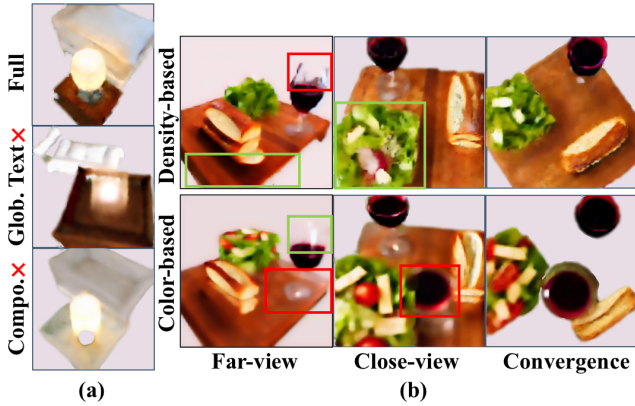


Figure 4: **The visual comparison of the impact of design choices.** (a) global text guidance(integrating local frames by Eq. (2)) and global calibration(integrating local frames, then aligning the rendering result directly with the full text). (b) comparison between color-based and density-based options.

both box and prompt guidance. Our framework, as shown in Fig. 3, applies the AABB ray intersection test algorithm to check for intersections on each box in the global frame. We then samples \mathbf{x}_g within the ray box intervals, and project them to \mathbf{x}_l to infer (C_l, σ_l) in separate NeRF models. We then utilize volume rendering to obtain rendered views for each local frame respectively. After that, they would be passed on to our tailored composition Module to infer (C_g, σ_g) for global rendering. Next, we match local and global texts with their corresponding image outputs by SDS losses. We also support recomposition by passing samples from cached models into \mathbf{x}_l to continue the above process.

Global Composition. Each local frame is optimized independently, causing a lack of global connections for scene composition. As shown in Fig. 4(a), we verify its necessity by dropping $\nabla \mathcal{L}_{\text{SDS}_g}$. Compared with our full model, its layout does not fit our shared sense of a room, *i.e.*, *nightstand* is usually lower than *bed*; *lamp* needs a base to support it. Additionally, it lacks global consistency, such as light reflection, to make it more realistic. Therefore, we leverage the full text semantics to ensure consistent global rendering across local frames. Instead of conditioning the global rendering view with the full prompt directly, we note that global calibration is necessary for geometry and color to be learned sufficiently. For example, we observe that geometric completeness and texture of *nightstand* are not ideal. Although reflection appears around *nightstand*, *bed* is stripped of the light. Therefore, we opt to leverage the correlation between the rendering output of the combined NeRFs and the overall semantics to perform multi-object scene reconstruction.

Before delving into module details, there are two choices (see Fig. 3) on the composition module design we need to elaborate on first. In Fig. 3, by taking \mathbf{x}_g into the composition module, their inferred properties are calibrated with gradients propagated from the global SDS loss. However, it remains unclear whether σ_g should be refined or not. The trade-off on its usage is the density adjustment bringing a

more reasonable layout and more geometric details that fit the global text prompt. While its potential downside is that C_g may not be optimal as σ_g has more uncertainty compared to σ_l , bringing sub-optimal rendering results.

We choose the density-based method after comparing them with the experiment shown in Fig. 4(b). Specifically, we test both designs on the scene *table wine* and discover that the density-based design provides more intrinsic details(as indicated by green boxes), *e.g.*, enriched wood grains, and a more natural shape for *salad* and has much faster convergence speed. In contrast, the color-based method enhances the reflection and smooths flickering on *wine cup*, (as indicated by red boxes), but it suffers from 1) sparse density, resulting in poorly generated geometry at the base of *cup* and the wood *table* corner. Additionally, shadow artifacts appeared on *table* when viewed up close, outweighing benefits of the color-based method.

Network Design. Fig. 3 depicts the network architecture of the composition module. Denote m as local MLP $\{\theta_l\}_{l=1}^m$ for each local frame. Then, we introduce the global MLPs including density θ_{gd} and θ_{gc} calibrators to refine σ_l and C_l . In detail, the network design is,

$$\sigma_g = \alpha_d \theta_{gd}(\sigma_l) + \sigma_l, \quad (4)$$

$$C_g = \alpha_c \theta_{gc}(C_l, d_g) + C_l, \quad (5)$$

where residual σ_l, C_l assist in learning σ_g and C_g , while α_d, α_c balance their contribution as learnable parameters. Note that the color-based omits density calibration, and simply uses the shared color refinement.

B. Recomposition Thanks to our CompoNeRF design, we can easily reconstruct scenes using available models. Additionally, it allows us to edit the boxes with $\{\theta_l\}_{l=1}^m$ before arranging them into a new layout. At Fig. 1, the input panel allows for editing of box positions, scales, and replacement with offline models. CompoNeRF enables scene-editing functions, such as text-editing, moving, scaling, and removing, as shown at Tab. 1. Furthermore, trained NeRFs can be decomposed and cached for other scenes.

C. Optimization After the multi-object volume rendering with Eq. (2), we match their rendering results with the corresponding text prompts, which is formulated as follows:

$$\mathcal{L} = \alpha_g \nabla \mathcal{L}_{\text{SDS}}(\hat{\mathbf{X}}_g, T) + \alpha_l \sum_{j=1}^m \nabla \mathcal{L}_{\text{SDS}}(\hat{\mathbf{X}}_{l,j}, T_{l,j}) + \beta \mathcal{L}_{\text{sparse}},$$

where T denotes the global text prompt, and T_l is a subset of T representing a single object. α_g, α_l , and β are hyper-parameters of loss weights. As suggested in (Metzer et al. 2022), we use $\mathcal{L}_{\text{sparse}}$ to penalize the binary entropy of local NeRF density and reduce the floating radiance clouds. Moreover, it's helpful to include a directional prompt like "front view" or "side view" in our input text similar to previous works (Poole et al. 2022; Metzer et al. 2022) to indicate global camera pose during training.

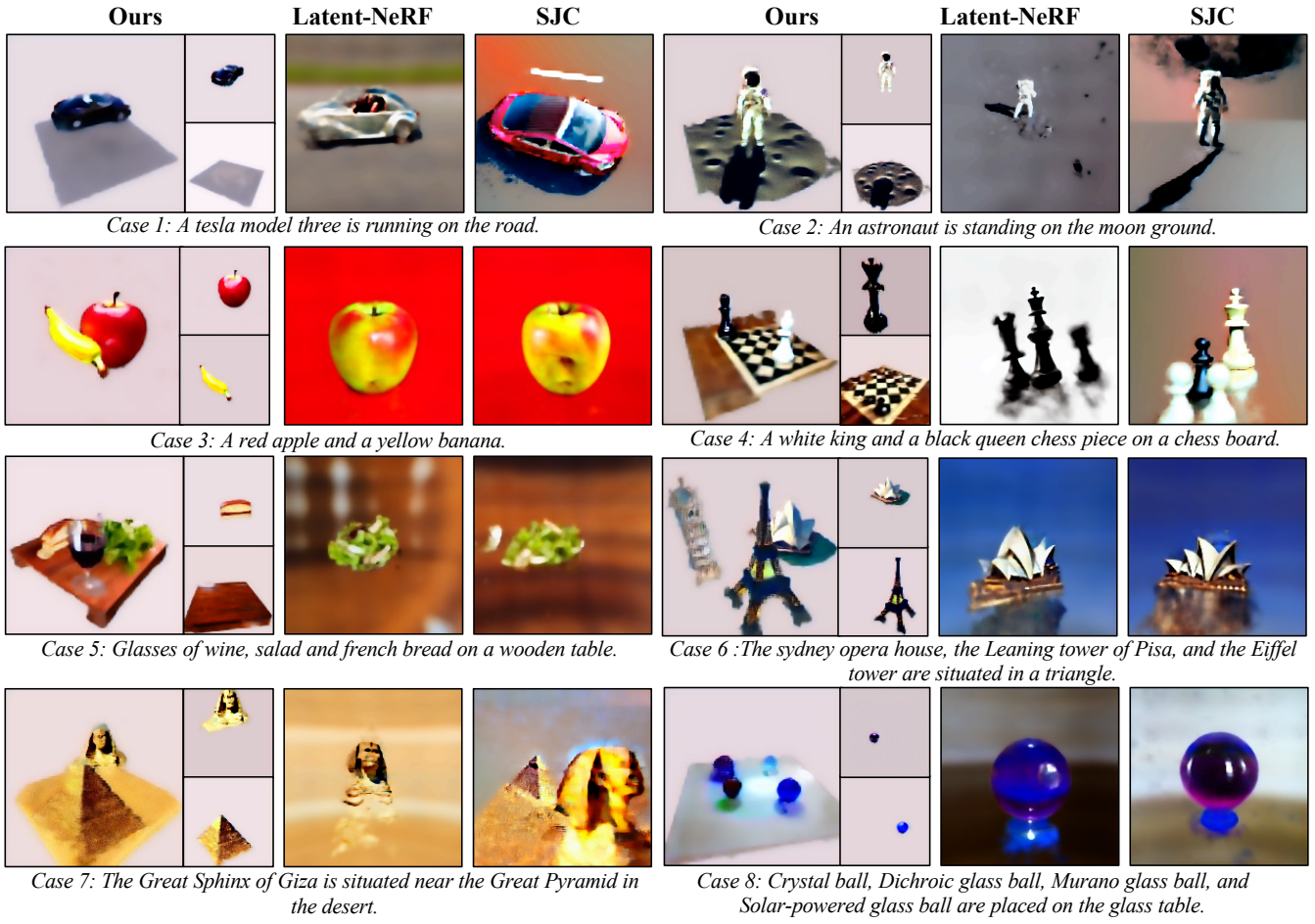


Figure 5: **Qualitative comparison with other text-to-3D methods using multi-object text prompts.** Case 1-3 represent easy settings with two-object compositions, while Cases 4-8 represent complex settings with more than two-object compositions. The small images next to our results depict the generated components (partially shown in Cases 4-8).

Method	Case 1	Case 2	Case 3	Case 4	Case 5	Case 6	Case 7	Case 8
LatentNeRF	25.16	27.07	27.69	31.19	21.55	26.32	27.43	29.51
SJC	23.55	27.84	28.21	30.53	23.33	27.41	25.62	28.76
CompoNeRF (Ours)	26.13	32.71	33.37	31.45	36.06	28.44	28.96	30.98

Table 2: **Performance comparison of our CompoNeRF in different 3D scenes.** We use CLIP score (Parmar et al. 2023; Zhang et al. 2023; Wang et al. 2023) as our evaluation metric, which is a common evaluation metric in text-to-image generation tasks to evaluate the similarity of the generated image to the text prompt.

4 Experiments

4.1 Implementation Details

For score distillation sampling, we use the v1-4 checkpoint of Stable Diffusion based on the latent diffusion model (Rombach et al. 2022). We utilize the codebase (Metzger et al. 2022) for 3D representation and grid encoder from Instant-NGP (Müller et al. 2022) as our NeRF model. The global MLP consists 4 or 6 Linear layers with 64 hidden channels. In the training loss, we set $\alpha_g = 100$, $\alpha_l = 50$, and $\beta = 5e^{-4}$. Our 3D scenes are optimized with a batch size of 1 using the Adam (Kingma and Ba 2014) optimizer

on a single RTX3090. See our *suppl.* for more details.

4.2 Qualitative Comparison

In Fig. 5, we present qualitative comparisons of generated 3D assets given the same multi-object text prompt with our proposed CompoNeRF method, as well as the Latent-NeRF and SJC, which are the SoTA methods based on the same Stable Diffusion model. We observe that our method can accurately generate complex 3D models across a diverse set of prompts with **precise object identity** and more **sensible and fertile context** than others in the showcases. For example, in the simple Case 3, our method accurately generates

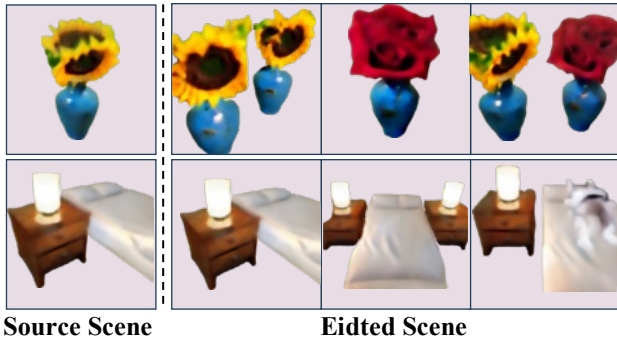


Figure 6: **Scene editing results** from manipulations on 3D layout, text prompt and scene recomposition.

two separate objects, a red *apple* and a yellow *banana*. In contrast, other methods generate a single mixed object with characteristics of both fruits. In the complex Case 5, we provide a realistic scene with accurate representations of *wine*, *table*, *salad*, *bread*, and *table*, including the glass reflection. However, other methods fail to generate even recognizable objects. Note that we cannot validate the predicted results of DreamFusion (Poole et al. 2022) and Magic3D (Lin et al. 2022) model as they are built upon on close-sourced diffusion models. Besides, our underlying 3D representation can also be equipped with most object-centric methods (Poole et al. 2022; Lin et al. 2022) once they are released to achieve, allowing us to achieve better single-object modeling, similar to the use of our Latent-NeRF backbone.

4.3 Quantitative Comparison

We use CLIP score as our evaluation metric to measure the similarity of generated 3D assets to text prompt. The CLIP score, a widely utilized evaluation metric in text-to-image generation tasks (Parmar et al. 2023; Zhang et al. 2023; Wang et al. 2023), is calculated as the cosine similarity between the embeddings of the text and image, both of which are encoded by the CLIP model. For 3D assets, we calculate the CLIP score between the projected images of the 3D assets and the prompt text in different views and take the average score as the overall CLIP score. In Tab. 2, we show quantitative comparison of the similarity between generated 3D assets and the same text prompt with the Latent-NeRF, SJC and our method across diverse scenes. As shown as Tab. 2, we achieve the best performance in all scenes, with more significant performance improvement in complex scenes. For example, in *table wine* scene, our method achieves a **54%** gain. **The excellent performance in complex scenes highlights the effectiveness of our global calibration.**

5 Discussion

Our proposed CompoNeRF method represents a preliminary step in handling multi-object text for text-to-3D generation. However, it unleashes its potential by composing scenes with reusable NeRF components, which also facilitates later editing. Nonetheless, we are unable to solve the

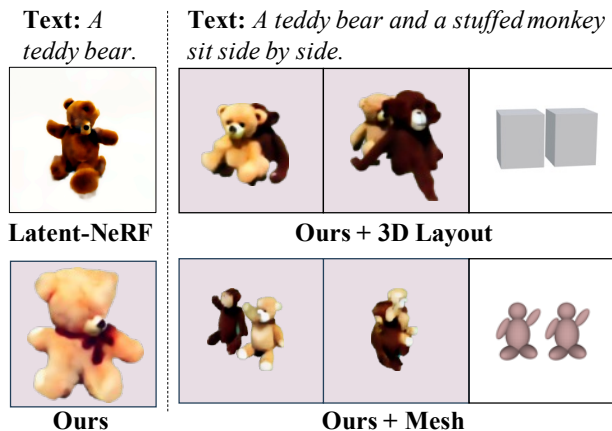


Figure 7: **(Left)** we observe the multi-face problem, *i.e.*, duplicated face views with geometry collapse in all methods, even in single-object cases. **(Right)** we provide mesh as guidance instead of box layouts to solve this problem, which further proves our method’s versatility and effectiveness.

multi-face problem in this paper since our box layout guidance is ambiguous for prompts with direction. In this section, we discuss these two points.

Editable Scene Rendering and Finetuning. Due to the compositional capacity brought by the editable 3D scene layout, we can perform scene editing by text editing, moving, scaling, duplicating, removing the single object, and recomposing a new scene by manipulating the layout of each learned local NeRF. Fig. 6 shows our edited scene rendering results based on a pre-trained scene. We can see that the manipulated objects are seamlessly integrated into the scene while ensuring the correct spatial relationship following the edited layout. For text editing on a specific object, we simply change a certain part of the text prompt, *e.g.*, ‘a vase of sunflower’ to ‘a vase of rose’ at both global and local text prompts and finetune the scene with a few steps. When moving and scaling existing objects, we only need to adjust the box property, such as the center point and box scale. As the duplication, removal, and recomposition, we can first input the 3D boxes and then load each box with a local text prompt from a learned local NeRF collection, *e.g.*, copy the single *nightstand* into the other at opposite locations. Furthermore, all types of manipulation can be combined together to generate a scene with multiple user control inputs.

Multi-face Problem and Stronger Prompt. Similar to Latent-NeRF and SJC, the guidance generated from Stable Diffusion may produce a multi-face problem for certain objects as shown in Fig. 7. The diffusion model can not guarantee to generate satisfactory guidance with the desired direction along with the sampling camera pose. An alternative to relieve the multi-face problem is adding stronger constraints to force the 3D representation to maintain geometric consistency. Our method also uses the mesh constraint, proposed by Latent-NeRF, as a more fine-grained 3D layout than the 3D box. Fig. 7 shows that the multi-face prob-

lem can be largely relieved with the more accurate mesh constraint. However, accurate mesh input requires extensive editing, which reduces practical values during application.

6 Conclusion and Future Work

In this work, we have proposed a multi-object text-guided compositional 3D scene generation framework, called CompoNeRF, based on an editable 3D scene layout. The 3D scene layout interpreted the multi-object text prompt as a set of local NeRFs binding with a spatial box and object-specific text prompt. The whole scene view is rendered by compositing local NeRFs defined in the layout. We also designed composition module and multi-level text guidance for improving the quality of generated 3D scenes. Despite that our flexible box layout may not be direction-aware that is unable to solve the multi-face problem, we have addressed the guidance collapse issue well in the multi-object scene reconstruction. Working with the large-scale Stable Diffusion model, we demonstrated that our method, the first attempt to adopt compositional NeRF design in the text-to-3D task, can generate compelling 3D models with multiple objects, comparing favorably to available concurrent works. Finally, we investigated an exciting application of our method for scene editing and reusing trained models for scene recomposition, identifying an avenue for future work.

References

Azinović, D.; Martin-Brualla, R.; Goldman, D. B.; Nießner, M.; and Thies, J. 2022. Neural RGB-D surface reconstruction. In *CVPR*, 6290–6301.

Barron, J. T.; Mildenhall, B.; Tancik, M.; Hedman, P.; Martin-Brualla, R.; and Srinivasan, P. P. 2021. Mip-NeRF: A Multiscale Representation for Anti-Aliasing Neural Radiance Fields. In *ICCV*, 5835–5844. IEEE.

Feng, W.; He, X.; Fu, T.-J.; Jampani, V.; Akula, A.; Narayana, P.; Basu, S.; Wang, X. E.; and Wang, W. Y. 2022. Training-Free Structured Diffusion Guidance for Compositional Text-to-Image Synthesis. *arXiv preprint arXiv:2212.05032*.

Gao, C.; Saraf, A.; Kopf, J.; and Huang, J.-B. 2021. Dynamic view synthesis from dynamic monocular video. In *ICCV*, 5712–5721.

Gao, J.; Shen, T.; Wang, Z.; Chen, W.; Yin, K.; Li, D.; Litany, O.; Gojcic, Z.; and Fidler, S. 2022. GET3D: A Generative Model of High Quality 3D Textured Shapes Learned from Images.

Guo, M.; Fathi, A.; Wu, J.; and Funkhouser, T. 2020. Object-centric neural scene rendering. *arXiv preprint arXiv:2012.08503*.

Ho, J.; Jain, A.; and Abbeel, P. 2020. Denoising diffusion probabilistic models. *Advances in Neural Information Processing Systems*, 33: 6840–6851.

Hong, F.; Zhang, M.; Pan, L.; Cai, Z.; Yang, L.; and Liu, Z. 2022. Avatarclip: Zero-shot text-driven generation and animation of 3d avatars. *arXiv preprint arXiv:2205.08535*.

Jain, A.; Mildenhall, B.; Barron, J. T.; Abbeel, P.; and Poole, B. 2022. Zero-shot text-guided object generation with dream fields. In *CVPR*, 867–876.

Kingma, D. P.; and Ba, J. 2014. Adam: A method for stochastic optimization. *arXiv preprint arXiv:1412.6980*.

Lee, H.-H.; and Chang, A. X. 2022. Understanding pure clip guidance for voxel grid nerf models. *arXiv preprint arXiv:2209.15172*.

Li, J.; Li, D.; Xiong, C.; and Hoi, S. 2022. Blip: Bootstrapping language-image pre-training for unified vision-language understanding and generation. In *ICML*, 12888–12900. PMLR.

Lin, C.-H.; Gao, J.; Tang, L.; Takikawa, T.; Zeng, X.; Huang, X.; Kreis, K.; Fidler, S.; Liu, M.-Y.; and Lin, T.-Y. 2022. Magic3D: High-Resolution Text-to-3D Content Creation. *arXiv preprint arXiv:2211.10440*.

Lindell, D. B.; Martel, J. N.; and Wetzstein, G. 2021. Autoint: Automatic integration for fast neural volume rendering. In *CVPR*, 14556–14565.

Liu, L.; Gu, J.; Lin, K. Z.; Chua, T.-S.; and Theobalt, C. 2020. Neural Sparse Voxel Fields. *ArXiv*, abs/2007.11571.

Liu, L.; Habermann, M.; Rudnev, V.; Sarkar, K.; Gu, J.; and Theobalt, C. 2021. Neural actor: Neural free-view synthesis of human actors with pose control. *ACM Transactions on Graphics (TOG)*, 40(6): 1–16.

Metzer, G.; Richardson, E.; Patashnik, O.; Giryes, R.; and Cohen-Or, D. 2022. Latent-NeRF for Shape-Guided Generation of 3D Shapes and Textures. *arXiv preprint arXiv:2211.07600*.

Mildenhall, B.; Srinivasan, P. P.; Tancik, M.; Barron, J. T.; Ramamoorthi, R.; and Ng, R. 2020a. NeRF: Representing Scenes as Neural Radiance Fields for View Synthesis. In *ECCV*.

Mildenhall, B.; Srinivasan, P. P.; Tancik, M.; Barron, J. T.; Ramamoorthi, R.; and Ng, R. 2020b. NeRF: Representing Scenes as Neural Radiance Fields for View Synthesis. In *ECCV*, volume 12346, 405–421. Springer.

Mirzaei, A.; Kant, Y.; Kelly, J.; and Gilitschenski, I. 2022. LaTeRF: Label and text driven object radiance fields. In *Computer Vision–ECCV 2022: 17th European Conference, Tel Aviv, Israel, October 23–27, 2022, Proceedings, Part III*, 20–36. Springer.

Mohammad Khalid, N.; Xie, T.; Belilovsky, E.; and Popa, T. 2022. CLIP-Mesh: Generating textured meshes from text using pretrained image-text models. In *SIGGRAPH Asia 2022 Conference Papers*, 1–8.

Müller, T.; Evans, A.; Schied, C.; and Keller, A. 2022. Instant neural graphics primitives with a multiresolution hash encoding. *arXiv preprint arXiv:2201.05989*.

Nichol, A. Q.; and Dhariwal, P. 2021. Improved denoising diffusion probabilistic models. In *ICML*, 8162–8171. PMLR.

Niemeyer, M.; and Geiger, A. 2021. Giraffe: Representing scenes as compositional generative neural feature fields. In *CVPR*, 11453–11464.

Ost, J.; Mannan, F.; Thuerey, N.; Knodt, J.; and Heide, F. 2021. Neural scene graphs for dynamic scenes. In *CVPR*, 2856–2865.

Parmar, G.; Kumar Singh, K.; Zhang, R.; Li, Y.; Lu, J.; and Zhu, J.-Y. 2023. Zero-shot image-to-image translation. In *ACM SIGGRAPH 2023 Conference Proceedings*, 1–11.

Poole, B.; Jain, A.; Barron, J. T.; and Mildenhall, B. 2022. Dreamfusion: Text-to-3d using 2d diffusion. *arXiv preprint arXiv:2209.14988*.

Pumarola, A.; Corona, E.; Pons-Moll, G.; and Moreno-Noguer, F. 2021. D-nerf: Neural radiance fields for dynamic scenes. In *CVPR*, 10318–10327.

Radford, A.; Kim, J. W.; Hallacy, C.; Ramesh, A.; Goh, G.; Agarwal, S.; Sastry, G.; Askell, A.; Mishkin, P.; Clark, J.; et al. 2021. Learning transferable visual models from natural language supervision. In *ICML*, 8748–8763. PMLR.

Raj, A.; Kaza, S.; Poole, B.; Niemeyer, M.; Ruiz, N.; Mildenhall, B.; Zada, S.; Aberman, K.; Rubinstein, M.; Barron, J.; et al. 2023. Dreambooth3d: Subject-driven text-to-3d generation. *arXiv preprint arXiv:2303.13508*.

Rombach, R.; Blattmann, A.; Lorenz, D.; Esser, P.; and Ommer, B. 2022. High-resolution image synthesis with latent diffusion models. In *CVPR*, 10684–10695.

Ruiz, N.; Li, Y.; Jampani, V.; Pritch, Y.; Rubinstein, M.; and Aberman, K. 2023. Dreambooth: Fine tuning text-to-image

diffusion models for subject-driven generation. In *Proceedings of the IEEE/CVF Conference on Computer Vision and Pattern Recognition*, 22500–22510.

Saharia, C.; Chan, W.; Saxena, S.; Li, L.; Whang, J.; Denton, E.; Ghasemipour, S. K. S.; Ayan, B. K.; Mahdavi, S. S.; Lopes, R. G.; et al. 2022. Photorealistic text-to-image diffusion models with deep language understanding. *arXiv preprint arXiv:2205.11487*.

Sanghi, A.; Chu, H.; Lambourne, J. G.; Wang, Y.; Cheng, C.-Y.; Fumero, M.; and Malekshan, K. R. 2022. Clip-forge: Towards zero-shot text-to-shape generation. In *CVPR*, 18603–18613.

Schuhmann, C.; Beaumont, R.; Vencu, R.; Gordon, C.; Wightman, R.; Cherti, M.; Coombes, T.; Katta, A.; Mullis, C.; Wortsman, M.; et al. 2022. Laion-5b: An open large-scale dataset for training next generation image-text models. *arXiv preprint arXiv:2210.08402*.

Song, Y.; Kong, C.; Lee, S.; Kwak, N.; and Lee, J. 2022. Towards Efficient Neural Scene Graphs by Learning Consistency Fields. *arXiv preprint arXiv:2210.04127*.

Srinivasan, P. P.; Deng, B.; Zhang, X.; Tancik, M.; Mildenhall, B.; and Barron, J. T. 2021. Nerv: Neural reflectance and visibility fields for relighting and view synthesis. In *CVPR*, 7495–7504.

Tretschk, E.; Tewari, A.; Golyanik, V.; Zollhöfer, M.; Lassner, C.; and Theobalt, C. 2021. Non-rigid neural radiance fields: Reconstruction and novel view synthesis of a dynamic scene from monocular video. In *ICCV*, 12959–12970.

Verbin, D.; Hedman, P.; Mildenhall, B.; Zickler, T. E.; Barron, J. T.; and Srinivasan, P. P. 2022. Ref-NeRF: Structured View-Dependent Appearance for Neural Radiance Fields. In *CVPR*, 5481–5490. IEEE.

Wang, C.; Chai, M.; He, M.; Chen, D.; and Liao, J. 2022a. Clip-nerf: Text-and-image driven manipulation of neural radiance fields. In *CVPR*, 3835–3844.

Wang, H.; Du, X.; Li, J.; Yeh, R. A.; and Shakhnarovich, G. 2022b. Score Jacobian Chaining: Lifting Pretrained 2D Diffusion Models for 3D Generation. *arXiv preprint arXiv:2212.00774*.

Wang, P.; Liu, L.; Liu, Y.; Theobalt, C.; Komura, T.; and Wang, W. 2021. NeuS: Learning Neural Implicit Surfaces by Volume Rendering for Multi-view Reconstruction. *Advances in Neural Information Processing Systems*, 34: 27171–27183.

Wang, S.; Saharia, C.; Montgomery, C.; Pont-Tuset, J.; Noy, S.; Pellegrini, S.; Onoe, Y.; Laszlo, S.; Fleet, D. J.; Soricut, R.; et al. 2023. Imagen editor and editbench: Advancing and evaluating text-guided image inpainting. In *Proceedings of the IEEE/CVF Conference on Computer Vision and Pattern Recognition*, 18359–18369.

Wu, Q.; Liu, X.; Chen, Y.; Li, K.; Zheng, C.; Cai, J.; and Zheng, J. 2022. Object-compositional neural implicit surfaces. In *Computer Vision–ECCV 2022: 17th European Conference, Tel Aviv, Israel, October 23–27, 2022, Proceedings, Part XXVII*, 197–213. Springer.

Xian, W.; Huang, J.-B.; Kopf, J.; and Kim, C. 2021. Space-time neural irradiance fields for free-viewpoint video. In *CVPR*, 9421–9431.

Xu, J.; Wang, X.; Cheng, W.; Cao, Y.-P.; Shan, Y.; Qie, X.; and Gao, S. 2022a. Dream3D: Zero-Shot Text-to-3D Synthesis Using 3D Shape Prior and Text-to-Image Diffusion Models. *arXiv preprint arXiv:2212.14704*.

Xu, Y.; Chai, M.; Shi, Z.; Peng, S.; Skorokhodov, I.; Siarohin, A.; Yang, C.; Shen, Y.; Lee, H.-Y.; Zhou, B.; et al. 2022b. DisCoScene: Spatially Disentangled Generative Radiance Fields for Controllable 3D-aware Scene Synthesis. *arXiv preprint arXiv:2212.11984*.

Yang, B.; Zhang, Y.; Xu, Y.; Li, Y.; Zhou, H.; Bao, H.; Zhang, G.; and Cui, Z. 2021. Learning object-compositional neural radiance field for editable scene rendering. In *ICCV*, 13779–13788.

Yu, C.; Zhou, Q.; Li, J.; Zhang, Z.; Wang, Z.; and Wang, F. 2023. Points-to-3D: Bridging the Gap between Sparse Points and Shape-Controllable Text-to-3D Generation. *arXiv preprint arXiv:2307.13908*.

Zhang, K.; Riegler, G.; Snavely, N.; and Koltun, V. 2020. NeRF++: Analyzing and Improving Neural Radiance Fields. *arXiv: CVPR*.

Zhang, X.; Srinivasan, P. P.; Deng, B.; Debevec, P.; Freeman, W. T.; and Barron, J. T. 2021. Nerfactor: Neural factorization of shape and reflectance under an unknown illumination. *ACM Transactions on Graphics (TOG)*, 40(6): 1–18.

Zhang, Z.; Han, L.; Ghosh, A.; Metaxas, D. N.; and Ren, J. 2023. Sine: Single image editing with text-to-image diffusion models. In *Proceedings of the IEEE/CVF Conference on Computer Vision and Pattern Recognition*, 6027–6037.

Zhi, S.; Laidlow, T.; Leutenegger, S.; and Davison, A. J. 2021. In-place scene labelling and understanding with implicit scene representation. In *ICCV*, 15838–15847.